Dalton Transactions

Accepted Manuscript

ROYAL SOCIETY OF CHEMISTRY

www.rsc.org/dalton

Metal−organic frameworks constructed from crown ether-based 1,4-benzenedicarboxylic acid derivatives

Teng-Hao Chen,[a] Andreas Schneemann,[b] Roland A. Fischer,[b] and Seth M. Cohen[a*]

[a] Department of Chemistry and Biochemistry, University of California, San Diego, La Jolla, California, 92093, USA

[b] Lehrstuhl für Anorganische Chemie II, Organometallics & Materials Chemistry, Ruhr-Universität Bochum, Universitätsstrase 150, 44801 Bochum, Germany

Abstract

A series of unprecedented crown ether- and thiacrown ether-derivatized benzene dicarboxylic acid (H_2bdc) ligands has been synthesized and incorporated into the prototype isoreticular metal−organic framework (IRMOF) and UiO-66 materials. In the case of UiO-66, only MOFs comprised from a mixed-ligand composition, requiring both unsubstituted bdc and crown ether containing ligands, could be prepared. These are among the few ligand derivatives, and resulting MOFs, that incorporate a macrocyclic group directly on the bdc ligand, providing a new, modular platform for exploring new supramolecular and coordination chemistry within MOFs.

Introduction

Metal−organic frameworks (MOFs) are widely studied porous materials with controllable functionality, and have been proposed for many industrial and technological applications.[1,2,3] Many efforts have been devoted to frameworks with ultrahigh porosity providing large-sized cavities or pore apertures for gas or guest molecule storage.[4,5] With the ability to construct MOFs with large cavities, bulky organic groups such as macrocyclic molecules have been introduced into these frameworks.[6] Macrocyclic molecules are widely studied in supramolecular chemistry as molecular cages, nanosized reaction vessels, switches and shuttles, liquid crystals, catalysts, and sensors.[7] To date, various macrocyclic linkers based on crown ethers,[8] azamacrocycles,[9] cyclodextrins,[10] pseudorotaxanes,[11] and rotaxanes[12] have been incorporated into MOFs. Crown ether-based linkers normally consist of flexible macrocyclic polyethers, which can form a complex with guest species through coordination or hydrogen bonds.[8] A flexible azamacrocyclic ligand has been used to construct a MOF which displayed a selective uptake of CO_2 over N_2.[13] Cyclodextrin-based MOFs have been fabricated from sugar-based, macrocyclic building blocks and have shown strong and reversible binding of CO_2.[14] Pseudorotaxane linkers enabled the resulting MOFs to exhibit specific stereoelectronic host-guest interactions, essential for the creation of solid-state molecular switches and molecular machines based on mechanically interlocked molecules.[15]

The difficult preparation of some macrocycles (high cost, low yield, multiple steps) has been improved by the development of C−C cross-coupling reactions and dynamic covalent chemistry.[16,17] However, incorporating small crown ethers, such as 12-crown-4, 15-crown-5, and 18-crown-6, into MOFs is still rare. Zhao and coworkers synthesized extended linear dicarboxylic acid ligands with 12-crown-4 or 15-crown-5 anchored (Fig. 1, ligand **1** and **2**).[18] These elongated linkers afforded interpenetrated structures, with frameworks that collapsed under vacuum activation. Park and Suh enhanced isosteric heat (Q_{st}) of H_2 adsorption by the entrapment of 15-crown-5 and 16-crown-6 ethers in a MOF.[19] Later, the same group designed an 18-crown-6-based tetradentate ligand (Fig. 1, ligand **3**), which could bind K^+, NH_4^+, and methyl viologen cations, for enhancing H_2 storage in the MOF.[8] In light of these prior studies, we sought to develop facile synthetic methods to generate various crown ether-based ligands for readily constructing robust MOFs. Herein, we report the design and synthesis of bdc derivatives containing 12-crown-4, 15-crown-5, and thiacrown ethers, and their resulting canonical IRMOF-

1 (also known as MOF-5 $[ZnO_4(bdc)_3]_n$; bdc^{2-} = 1,4-benzenedicarboxylate) and UiO-66 (University of Oslo, $[Zr_6(OH)_4O_4(bdc)_6]_n$) structures. These studies provide a fundamental understanding on the incorporation of crown ether-based linkers into MOFs and shed light on the design of robust crown ether MOFs for selective metal binding or molecular separations.

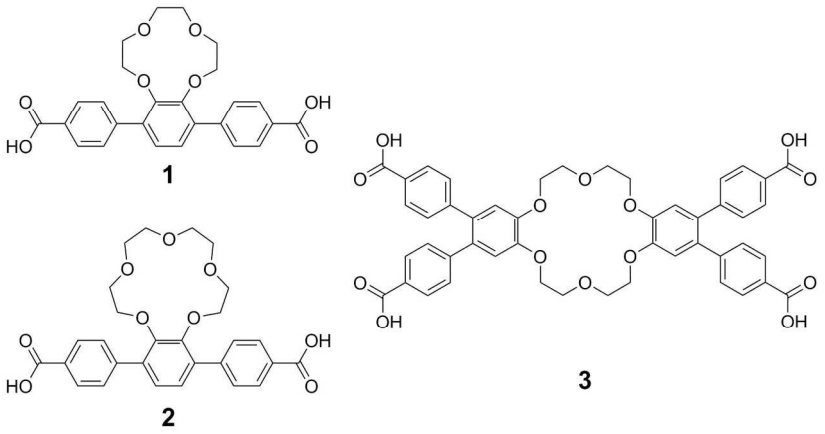

Fig. 1 Previous examples of small crown ether-appended ligands used for MOF synthesis.

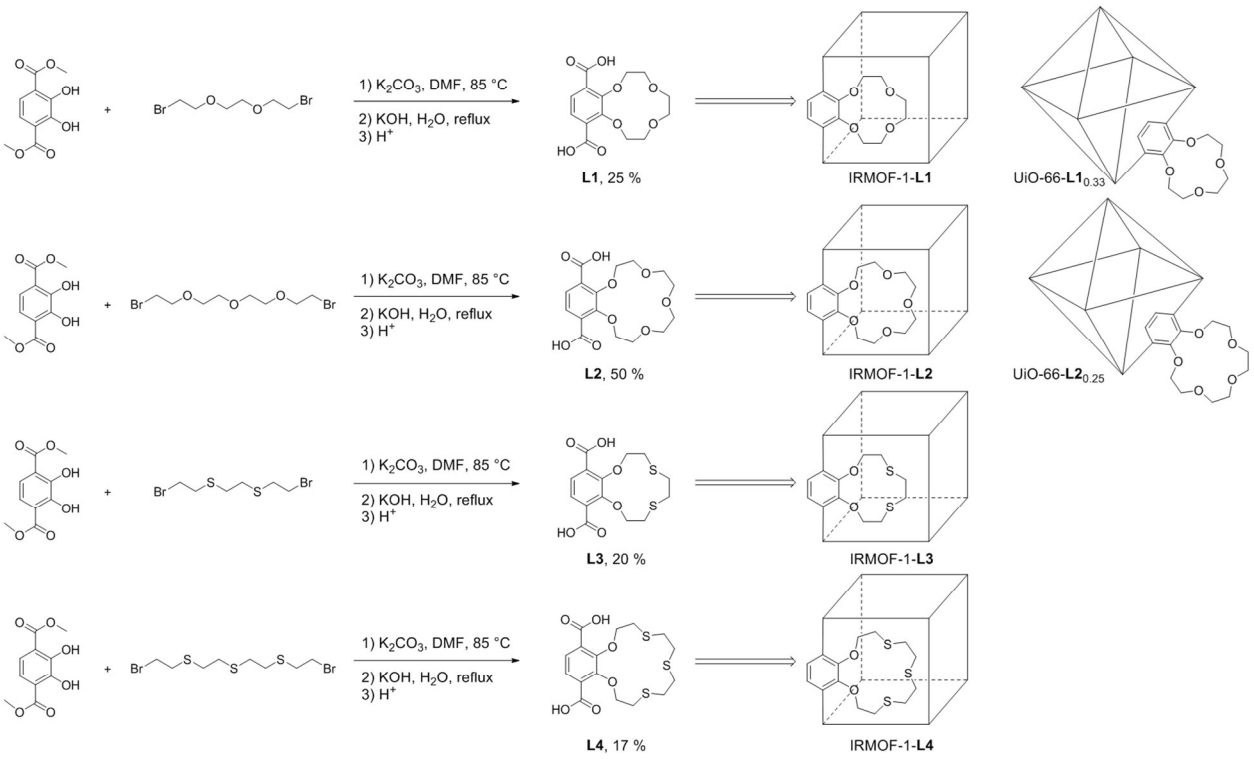

Scheme 1 Synthetic scheme for crown ether- and thiacrown ether-based ligands and resulting MOFs.

Experimental

General. Starting materials and solvents were purchased and used without further purification from commercial suppliers (Sigma-Aldrich, Alfa Aesar, EMD, TCI, and others). Chromatography was performed using a CombiFlash Rf 200 automated system from TeledyneISCO (Lincoln, USA). ^{1}H and ^{13}C nuclear magnetic resonance (NMR) spectra were collected on Varian Mercury spectrometers running at 400 and 500 MHz, respectively. Chemical shifts are quoted in parts per million (ppm) referenced to the appropriate solvent peak or 0 ppm for TMS. Electrospray ionization mass spectrometry (ESI-MS) was performed at the Molecular Mass Spectrometry Facility (MMSF) in the Department of Chemistry & Biochemistry at the University of California, San Diego. Elemental analysis was carried out at the NuMega Resonance Labs, Inc.

General Synthesis for Compounds H_2L1−H_2L4. Anhydrous potassium carbonate (1.10 g, 7.90 mmol) and dimethyl-2,3-dihydroxyterephthalate[20] (1.50 g, 6.64 mmol) were dissolved in 100 mL of *N,N*-dimethylformamide (DMF). Under vigorous stirring a dibromoalkylether compound (6.64 mmol, Scheme 1) was added (see Supporting Information for details). The mixture was heated at 85 °C overnight and was then filtered to remove K_2CO_3. DMF in the mixture was removed in vacuo by rotary evaporation. The remainder was purified by silica gel column chromatography (hexane/ethyl acetate gradient: 80/20 to 40/60) and the solvent from the appropriate fractions was removed under vacuum by rotary evaporation. Water (100 mL) and KOH (600 mg) were added to the resulting solid and the solution was heated to reflux overnight. After cooling down to room temperature, the solution was acidified with 1M HCl in an ice bath. The solution became turbid, but no significant precipitation was observed. The volume of water was reduced to below 5 mL under vacuum and an off-white solid precipitated upon cooling in an ice bath. The precipitate was filtered off, washed with water (100 mL), and dried overnight in vacuo.

L1. Yield: 0.51 g (25%). ^{1}H NMR (400 MHz, DMSO-d_6): δ 7.43 (s, 2H, ArH), 4.14 (t, 4H, CH_2, J = 6 Hz), 3.77 (t, 4H, CH_2, J = 6 Hz), 3.66 (s, 4H, CH_2). ^{13}C NMR (125 MHz, DMSO-d_6): 167.1, 152.5, 131.1, 125.1, 74.5, 70.8, 70.0. ESI-MS(−): calculated m/z = 311.08 $[M - H]^-$, observed m/z = 311.07.

L2. Yield: 1.17 g (50%). ^{1}H NMR (400 MHz, DMSO-d_6): δ 7.38 (s, 2H, ArH), 4.10 (t, 4H, CH_2, J = 6 Hz), 3.82 (t, 4H, CH_2, J = 6 Hz), 3.60 (s, 8H, CH_2). ^{13}C NMR (125 MHz, DMSO-d_6):

167.2, 152.3, 131.0, 124.9, 74.2, 70.8, 70.0, 69.9. ESI-MS(−): calculated *m/z* = 355.10 $[M - H]^-$, observed *m/z* = 355.02.

L3. Yield: 0.44 g (20%). ^{1}H NMR (400 MHz, DMSO-d_6): δ 7.46 (s, 2H, ArH), 4.28 (t, 4H, CH_2, *J* = 5.5 Hz), 3.04 (t, 4H, CH_2, *J* = 5.5 Hz), 2.97 (s, 4H, CH_2). ^{13}C NMR (125 MHz, DMSO-d_6): 167.0, 152.3, 130.2, 125.4, 77.5, 33.0, 32.2. ESI-MS(−): calculated *m/z* = 343.03 $[M - H]^-$, observed *m/z* = 342.95.

L4. Yield: 0.45 g (17%). ^{1}H NMR (400 MHz, DMSO-d_6): δ 7.44 (s, 2H, ArH), 4.13 (t, 4H, CH_2, *J* = 8 Hz), 2.95 (t, 4H, CH_2, *J* = 8 Hz), 2.83 (t, 4H, CH_2, *J* = 8 Hz), 2.80 (s, 4H, CH_2, *J* = 8 Hz). ^{13}C NMR (125 MHz, DMSO-d_6): 167.0, 151.6, 131.1, 125.3, 74.3, 32.0, 30.7, 30.6. ESI-MS(−): calculated *m/z* = 403.03 $[M - H]^-$, observed *m/z* = 402.97.

MOF Synthesis. *Syntheses of IRMOF-1-**L1** ($[ZnO_4(\mathbf{L1})_3]_n$), IRMOF-1-**L2** ($[ZnO_4(\mathbf{L2})_3]_n$), IRMOF-1-**L3** ($[ZnO_4(\mathbf{L3})_3]_n$), and IRMOF-1-**L4** ($[ZnO_4(\mathbf{L4})_3]_n$).* $Zn(NO_3)_2 \cdot 6H_2O$ (75 mg, 0.24 mmol) and a crown ether bdc ligand (**L1**, **L2**, **L3**, **L4**, 0.08 mmol) were dissolved in 8 mL of DMF in a 20 mL scintillation vial. The vial was placed in a sand bath in a preheated isothermal oven at 100 °C for 24 h. The mother liquor was decanted, and the resulting colorless crystals were washed with DMF (3×10 mL), rinsed with dichloromethane (CH_2Cl_2, 3×10 mL), and soaked for 3 d in CH_2Cl_2, which was replaced with fresh solvent every 24 h. The crystals were stored in CH_2Cl_2 until needed. Yield: IRMOF-1-**L1** 22 mg (67%), IRMOF-1-**L2** 22 mg (62%), IRMOF-1-**L3** 25 mg (75%), and IRMOF-1-**L4** 28 mg (77%).

*Syntheses of UiO-66-**L1**$_{0.33}$ and UiO-66-**L2**$_{0.25}$.* $ZrCl_4$ (250 mg, 1.10 mmol), H_2bdc (90 mg, 0.55 mmol), and a crown ether bdc ligand (**L1**, **L2**, 0.55 mmol) were dissolved in 40 mL of DMF and 9.5 mL of acetic acid in a 100 mL scintillation bottle. The vial was placed in a sand bath in a preheated isothermal oven at 120 °C for 24 h. After cooling, the solids were isolated via centrifugation at 6,000 rpm for 15 min using a fixed angle rotor, and washed thoroughly with fresh DMF (3×20 mL). The solid was left to soak in CH_2Cl_2 for 3 d, and the liquid was replaced with fresh CH_2Cl_2 (20 mL) every 24 h. After 3 d of soaking, the solid was isolated via centrifugation (6,000 rpm for 15 min using a fixed angle roto), and dried under vacuum. Yield: UiO-66-$\mathbf{L1}_{0.33}$ 256 mg (71%) and UiO-66-$\mathbf{L2}_{0.25}$ 240 mg (68%).

Analysis by ^{1}H NMR. For IRMOFs, ~5 mg of dried solid was digested with sonication in 500 μL of DMSO-d_6 and 5 μL of 35% DCl in D_2O. For UiO-66 MOFs, ~5 mg of dried solid was digested with sonication in 500 μL of DMSO-d_6 and 5 μL of 40% HF.

Thermal Analysis. ~5−10 mg of dried MOF material was used for thermogravimetric analysis (TGA) measurements. Samples were analyzed under a stream of dinitrogen (80 mL/min) using a Mettler Toledo TGA/DSC 1 STAR^e System running from 30 to 800 °C with a ramping rate of 5 °C/min.

PXRD Analysis. ~15−30 mg of MOF was filtered and air-dried (~5 min) before powder X-ray diffraction (PXRD) analysis. PXRD data were collected at ambient temperature on a Bruker D8 Advance diffractometer using a LynxEye detector at 40 kV and 40 mA for Cu Kα (λ = 1.5418 Å), with a scan speed of 1 s/step, a step size of 0.02 in 2θ, and a 2θ range of 5−40°.

Gas Sorption Analysis. All gases used were of 99.999% purity. ~50−100 mg of MOF (soaking in CH_2Cl_2) was transferred to a pre-weighed sample tube and evacuated on a vacuum line for 10 min at room temperature. The sample was then degassed at 150 °C on a Micromeritics ASAP 2020 Adsorption analyzer for a minimum of 10 h. The sample tube was re-weighed to obtain a consistent mass of the degassed sample. Brunauer-Emmett-Teller (BET) surface area measurements (m^2/g) were collected on three independent samples at 77 K with N_2 on the same instrument using the volumetric technique. The Q_{st} of H_2 adsorption was estimated from the H_2 sorption data measured at 77 K and 87 K. The data were fit to virial-type equations according to literature.[8]

Scanning Electron Microscopy. MOFs were transferred to conductive carbon tape on a sample holder disk, and coated by Ir-sputtering for 7 sec. A Philips XL ESEM instrument was used for acquiring images using a 10 kV energy source under vacuum at a working distance of 10 mm.

Results and Discussion

The focus of this study was to synthesize prototypical frameworks, such as IRMOF-1 and UiO-66, using crown ether-appended bdc ligands. Combining dimethyl-2,3-dihydroxyterephthalate[20] with various dibromoalkyl ether compounds (Scheme 1, see Supporting Information for details), we were able to synthesize compounds **L1**−**L4** via the Williamson ether synthesis in yields ranging from 17−50%.[21] To the best of our knowledge, **L3** and **L4** are the first examples of sulfur-containing crown ether ligands to be employed for MOF synthesis.

Using conventional solvothermal conditions, the desired IRMOF analogues (IRMOF-1-**L1**−**L4**) were obtained as block-shape crystals. These crystals exhibited PXRD patterns as

expected for an IRMOF lattice (Fig. 2). Noticeably, the peak at $2\theta = 9.7°$ splits in the PXRD pattern of IRMOF-1-**L2**. This phenomenon was also observed and described in studies of IRMOF-1 when the pores were occupied by organic and inorganic species.[22] The crown ether group of **L2** and trapped solvent molecules might contribute to the peak splitting in the PXRD of IRMOF-1-**L2**. The sizes of the crystals of IRMOF-1-**L1** and -**L2** were large enough ($>0.05\times0.05\times0.05$ mm^3) for single crystal X-ray diffraction analysis. However, under polarized light, the crystals showed polycrystalline features (Fig. S19, S20) and suitable single crystal X-ray diffraction data could not be obtained. The tiny crystals of IRMOF-1-**L3** and -**L4** were also polycrystalline as confirmed by SEM (Fig. S23). However, the PXRD data (Figure 2) unambiguously show that these materials possess the canonical IRMOF architecture.

For the synthesis of MOFs with the UiO-66 architecture, starting with 1:1 molar ratio of $ZrCl_4$ and **L1** or **L2** under solvothermal conditions, amorphous white powders were obtained (Fig. S24, S25). Keeping the 1:1 molar ratio of $ZrCl_4$ to ligand, and adjusting the ratio between bdc and **L1** or **L2**, allowed the formation of crystalline compounds when the ratio of bdc:**L1** (or **L2**) was 1:1 (Fig. 1). SEM images revealed the octahedral morphology, typical of the UiO-66 framework (Fig. S26).[23] After digestion of the resulting MOFs in HF/D_2O solution, the framework constructed from bdc and **L1** was found to contain 33% of **L1** (Fig. S27), while the product from bdc and **L2** was found to contain 25% of **L2** (Fig. S28). Thus, we denoted these frameworks as UiO-66-**L1**$_{0.33}$ and UiO-66-**L2**$_{0.25}$. For **L3** and **L4**, despite numerous attempts, under a variety of solvothermal conditions, no crystalline product was obtained with $ZrCl_4$, perhaps due to coordination of the thiacrown ether to Zr(IV).[24] Adding more equivalents of **L3** or **L4** produced white precipitates, but the products were amorphous as confirmed by PXRD (data not shown). Postsynthetic exchange (PSE) of **L3** or **L4** into as-synthesized UiO-66 was also unsuccessful in our hands (data not shown).[25]

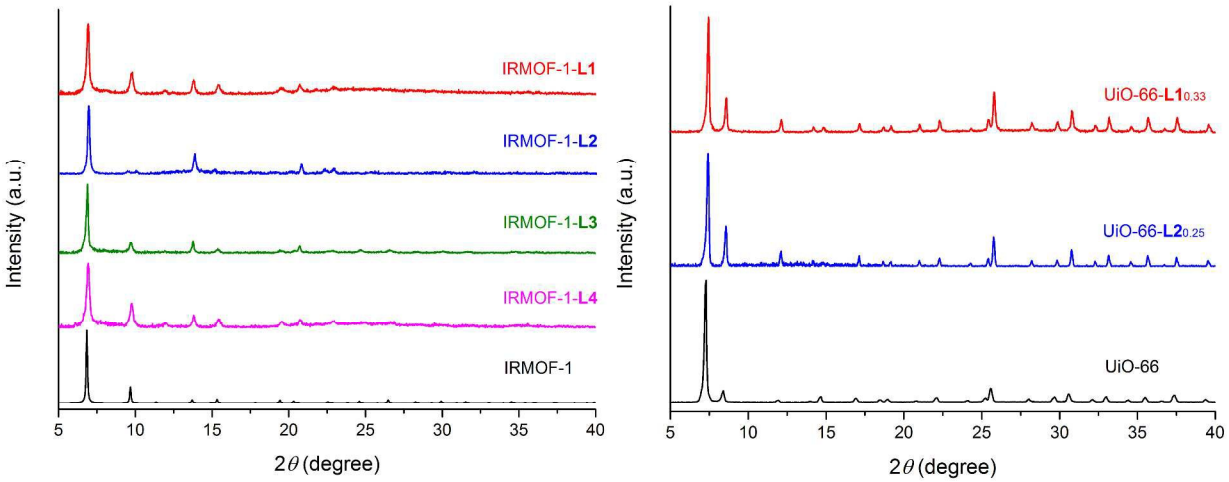

Fig. 2 PXRD of IRMOF-1-**L1**−**L4** (left), and UiO-66-**L1**$_{0.33}$ and –**L2**$_{0.25}$ (right) after air-drying from DMF.

TGA analysis showed similar results for all of the crown ether-based MOFs. Although the solids were activated at 150 °C in vacuum for 10 h before the measurements, the TGA data (Figure 3) indicated obvious weight losses below 100 °C suggesting that certain amounts of water from the atmosphere were adsorbed by the hydrophilic crown ether groups during the sample preparation. These materials began to decompose between 220 and 260 °C. We attribute the low decomposition temperature to the degradation of crown ether units. The elemental analysis reveals that the activated materials (Table S1) contain 24−38 wt% carbon, which is 4−15 wt% less than the calculated values according to the theoretical formulas. Presumably, this is due to a certain amount of metals trapped either in the pores of the frameworks or in the cavities of crown ethers or thiacrown ethers. Especially for IRMOF-1-**L3** and -**L4**, the complex ^{1}H NMR spectra of the crystals digested in DCl/D_2O (Fig. S29, S30) showed multiple broad peaks indicating a strong coordination between Zn(II) cations and thiacrown ethers.[26] In case of UiO-66-**L1**$_{0.33}$ and UiO-66-**L2**$_{0.25}$, it is well-known that Zr-based MOFs commonly display defects where some organic linkers in the structure may be missing.[27] This may also account for the large discrepancy between the experimental and calculated values of elemental analysis, especially when bulky crown ether ligands are incorporated.

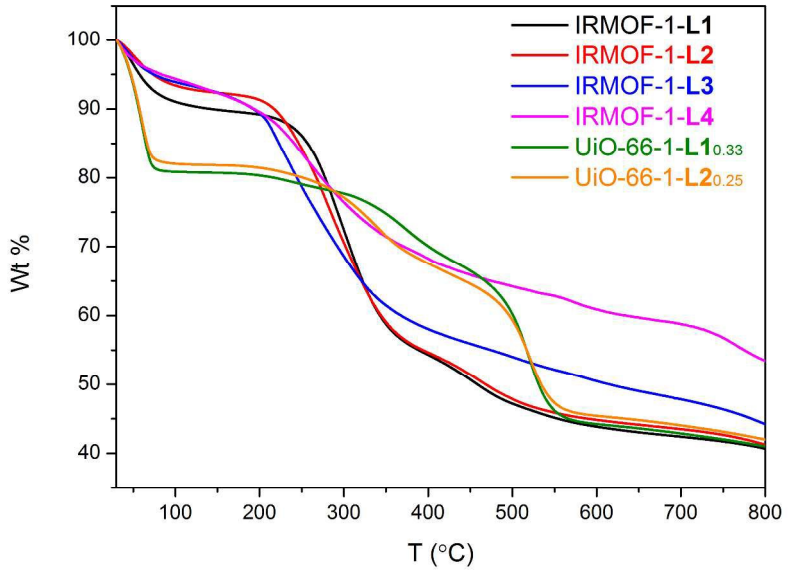

Fig. 3 TGA traces for IRMOF-1-**L1**–**L4** and UiO-66-**L1**$_{0.33}$–**L2**$_{0.25}$.

IRMOF-1-**L1** and -**L2** exhibited BET surface areas of 1204 and 899 m^2/g, respectively, after activation at 150 °C under vacuum (Fig. 4). These BET surface areas are significantly lower than that of IRMOF-1, but consistent with the porous MOF architecture. The reduced surface areas are likely attributable to the bulky crown ether groups. The frameworks of IRMOF-1-**L3** and -**L4** collapsed after activation at both room temperature and 150 °C (Fig. S31), which hindered further surface area analysis. The BET surface areas of UiO-66-**L1**$_{0.33}$ and UiO-66-**L2**$_{0.25}$ were 999 and 795 m^2/g, respectively (Fig. 4, right). The trend of decreasing surface areas due to incorporation of bulkier ligands observed in the UiO-66 series is consistent with that of IRMOF-1-**L1** and -**L2**, as well as many other reports on similar systems.[19]

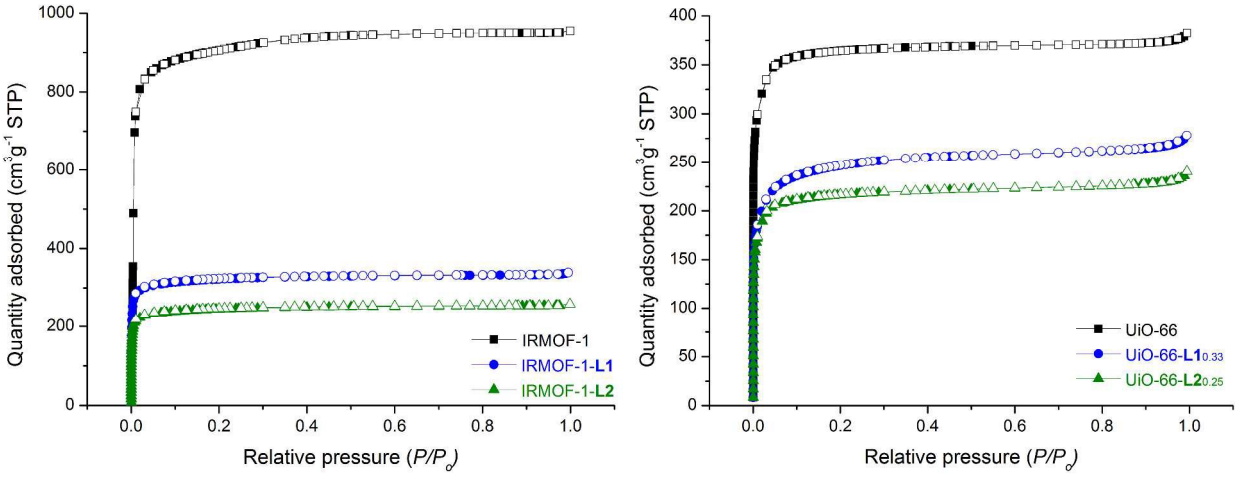

Fig. 4 N_2 sorption isotherms of IRMOF-1-**L1** and IRMOF-1-**L2** (left) at 77 K. N_2 sorption isotherms of UiO-66-**L1**$_{0.33}$ and UiO-66-**L2**$_{0.25}$ (right) at 77 K. Samples were activated at 150 °C under vacuum. Filled symbols are the adsorption curves; open symbols are the desorption curves.

The four MOFs that displayed appreciable surface areas were also examined for H_2 adsorption. The zero-coverage isosteric heat (Q_{st}) of the H_2 adsorption was estimated from the H_2 adsorption isotherms measured at 77 K and 87 K under 1 atm using virial equation (Fig. 5).[8] The total amounts of H_2 uptake in these MOFs are less than those of their parent MOFs, IRMOF-1 (Fig. 5a) and UiO-66 (Fig. 5b), again likely due to the incorporation of bulky crown ethers. IRMOF-1-**L1** and -**L2** have approximately one-third the BET surface area of IRMOF-1, but their H_2 uptakes at 77 K are only 16 and 33% less than that of IRMOF-1. Interestingly, the calculated Q_{st} values of H_2 adsorption of these four materials are slightly higher than those of the parent MOFs (Fig. 5c, Table S2, S3). For IRMOF-1-**L2** the Q_{st} value (6.52 kJ/mol) is 26% higher than that of IRMOF-1 (5.16 kJ/mol), and this observation is comparable to other crown ether-derivatized MOFs.[19]

Because crown ethers are able to selectively bind alkali metal ions,[28] which are predicted to help enhance H_2 storage in MOFs,[29] we further tried to metalate IRMOF-1-**L1**, IRMOF-1-**L2**, UiO-66-**L1**$_{0.33}$, and UiO-66-**L2**$_{0.25}$. **L1**- and **L2**-based MOFs were exposed to 0.1 M $LiNO_3$/DMF and $NaNO_3$/DMF solution, respectively, at room temperature for 1 d and then washed with DMF. After solvent exchange with CH_2Cl_2 for 3 d, the materials were activated at 150 °C under vacuum. The PXRD patterns (Fig. S32, S33) and N_2 77 K adsorption isotherms (Fig. S34) confirmed the maintenance of crystallinity and porosity after activation. As controls,

their parent MOFs (IRMOF-1 and UiO-66) were also treated under the same metalation conditions. The PXRD data indicated that IRMOF-1 lost its crystallinity after the metalation treatment, while UiO-66 remained crystalline (Fig. S32, S33). These results reveal that the MOFs composed of compact crown ether ligands are stable in the alkali-metal-containing solutions and remain intact even after conventional activation. The four activated crown ether MOFs after metalation were examined for H_2 adsorption. However, the Q_{st} of H_2 adsorption of the resulting materials did not display any significant improvement. Other metalation conditions were explored (e.g. different metal salts, solvents, temperatures, see Table S2, S3) but none resulted in materials with enhanced H_2 sorption. Furthermore, the inductively coupled plasma-optical emission spectrometry (ICP-OES) analysis of these MOFs indicated no significant uptake of lithium or sodium cations in the frameworks. These results suggest that the crown ether MOFs were not efficiently metalated under the reaction conditions explored here. The metal-binding ability of the free ligands was examined by dissolving **L1** and **L2** in DMSO-d_6 and titrating in excess equivalents of alkali metals; however, no chemical shift was observed in the ^{1}H NMR spectra (Fig. S35 and S36). In contrast, compounds **1** and **2** (Figure 1) showed significant changes in chemical shift when treated with alkali metal-containing solutions.[18] It may be that the electron-withdrawing carboxylic acid groups adjacent to the crown ether in **L1** and **L2** substantially decrease the metal-binding ability of these crown ether ligands.

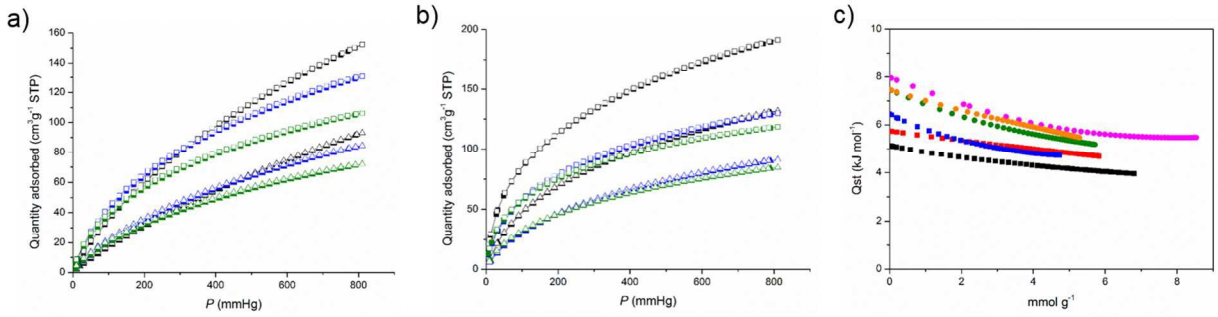

Fig. 5 H_2 sorption isotherms at 77 K (square) and 87 K (triangle); a) Black: IRMOF-1, blue: IRMOF-1-**L1**, and green: IRMOF-1-**L2**; b) black: UiO-66, blue: UiO-66-**L1**$_{0.33}$, and green: UiO-66-**L2**$_{0.25}$. Filled shape: adsorption; open shape: desorption. c) Isosteric heat (Q_{st}) of H_2 adsorption; black: IRMOF-1, red: IRMOF-1-**L1**, blue: IRMOF-1-**L2**, green: UiO-66, magenta: UiO-66-**L1**$_{0.33}$, and orange: UiO-66-**L2**$_{0.25}$.

Conclusion

In this study, we have synthesized a variety of novel crown ether-appended bdc ligands that can be incorporated into prototypical MOFs. **L1**−**L4** are able to combine with Zn(II) to form IRMOF-1 architectures. The bulkiness of crown ether groups and the relatively small pores of UiO-66 framework permitted the synthesis of UiO-66 analogues only from combinations of bdc and crown ether-substituted bdc (**L1** and **L2**) ligands. Ligands **L3** and **L4**, containing soft sulfur heteroatoms, appear to hinder the formation of UiO-66 architecture. Unlike most of the crown ether-containing MOFs that have been reported, the MOFs constructed from **L1** and **L2** show high stability toward conventional activation at high temperatures under vacuum and metalation treatment. Although the crown ether MOFs appeared unable to bind alkali-metals which could enhance hydrogen storage, these crown ether ligands may be of interest for host-guest chemistry within MOFs. This work provides a route to incorporate the fundamental units of supramolecular chemistry into MOFs. Combining macrocyclic groups with modular architectures of MOFs could potentially lead to interesting applications in guest molecule capture and separations.[30, 31]

ASSOCIATED CONTENT

Supporting Information

Synthesis and characterization of starting materials and MOFs. This material is available free of charge via the internet at http://pubs.acs.org.

AUTHOR INFORMATION

Corresponding authors

*E-mail: scohen@ucsd.edu. Telephone: (858) 822-5596

Funding

This work was supported by a grant from the Department of Energy, Office of Basic Energy Sciences, Division of Materials Science and Engineering under Award No. DE-FG02-08ER46519. A.S. gratefully acknowledges the German Academic Exchange Service (DAAD) for a 6-month visiting graduate fellowship to conduct research at UC San Diego. A.S. furthermore acknowledges the research cluster SusChemSys for a doctoral fellowship. The project “Sustainable Chemical Synthesis (SusChemSys)” is co-financed by the European

Regional Development Fund (ERDF) and the state of North Rhine-Westphalia, Germany, under the Operational Programme “Regional Competitiveness and Employment” 2007–2013.

Notes

The authors declare no competing financial interests.

ACKNOWLEDGEMENTS

We thank the Molecular Mass Spectrometry Facility (Dr. Yongxuan Su, UC San Diego) for assistance with the MS experiments, and Prof. Paterno Castillo and Dr. Christopher MacIsaac (Scripps Institution of Oceanography, UC San Diego) for assistance with the ICP-OES experiments.

REFERENCES

1. Z. W. W. Lu, Z.-Y. Gu, T.-F. Liu, J. Park, J. Park, J. Tian, M. Zhang, Q. Zhang, T. Gentle III, M. Boscha and H.-C. Zhou, *Chem. Soc. Rev.*, 2014, **43**, 5561−5593.
2. A. G. Slater and A. I. Cooper, *Science*, 2015, **348**.
3. A. Schneemann, S. Henke, I. Schwedler and R. A. Fischer, *ChemPhysChem*, 2014, **15**, 823−839.
4. T. C. Wang, W. Bury, D. A. Gómez-Gualdrón, N. A. Vermeulen, J. E. Mondloch, P. Deria, K. Zhang, P. Z. Moghadam, A. A. Sarjeant, R. Q. Snurr, J. F. Stoddart, J. T. Hupp and O. K. Farha, *J. Am. Chem. Soc.*, 2015, **137**, 3585−3591.
5. H. Deng, S. Grunder, K. E. Cordova, C. Valente, H. Furukawa, M. Hmadeh, F. Gándara, A. C. Whalley, Z. Liu, S. Asahina, H. Kazumori, M. O’Keeffe, O. Terasaki, J. F. Stoddart and O. M. Yaghi, *Science*, 2012, **336**, 1018−1023.
6. H. Zhang, R. Zou and Y. Zhao, *Coord. Chem. Rev.*, 2015, **292**, 74−90.
7. F. Davis and S. Higson, *Macrocycles: Construction, Chemistry and Nanotechnology Applications*, Wiley: A John Wiley and Sons, Ltd., Publication, 2011.
8. D.-W. Lim, S. A. Chyun and M. P. Suh, *Angew. Chem., Int. Ed.*, 2014, **53**, 7819−7822.
9. S. Tashiro, R. Kubota and M. Shionoya, *J. Am. Chem. Soc.*, 2012, **134**, 2461−2464.
10. R. A. Smaldone, R. S. Forgan, H. Furukawa, J. J. Gassensmith, A. M. Z. Slawin, O. M. Yaghi and J. F. Stoddart, *Angew. Chem., Int. Ed.*, 2010, **49**, 8630−8634.

11. Q. Li, W. Zhang, O. Š. Miljanić, C.-H. Sue, Y.-L. Zhao, L. Liu, C. B. Knobler, J. F. Stoddart and O. M. Yaghi, *Science*, 2009, **325**, 855−859.
12. V. N. Vukotic, K. J. Harris, K. Zhu, R. W. Schurko and S. J. Loeb, *Nat. Chem.*, 2012, **4**, 456−460.
13. W.-Y. Gao, Y. Niu, Y. Chen, L. Wojtas, J. Cai, Y.-S. Chen and S. Ma, *CrystEngComm*, 2012, **14**, 6115−6117.
14. J. J. Gassensmith, H. Furukawa, R. A. Smaldone, R. S. Forgan, Y. Y. Botros, O. M. Yaghi and J. F. Stoddart, *J. Am. Chem. Soc.*, 2011, **133**, 15312−15315.
15. K. Zhu, C. A. O'Keefe, V. N. Vukotic, R. W. Schurko and S. J. Loeb, *Nat. Chem.*, 2015, **7**, 514−519.
16. T.-H. Chen, I. Popov, Y.-C. Chuang, Y.-S. Chen and O. Š. Miljanić, *Chem. Commun.*, 2015, **51**, 6340−6342.
17. W. Zhang and J. S. Moore, *Angew. Chem., Int. Ed.*, 2006, **45**, 4416−4439.
18. L. Liu, X. Wang, Q. Zhang, Q. Li and Y. Zhao, *CrystEngComm*, 2013, **15**, 841−844.
19. H. J. Park and M. P. Suh, *Chem. Commun.*, 2012, **48**, 3400−3402.
20. K. K. Tanabe, C. A. Allen and S. M. Cohen, *Angew. Chem., Int. Ed.*, 2010, **49**, 9730−9733.
21. C. A. Allen and S. M. Cohen, *Inorg. Chem.*, 2014, **53**, 7014−7019.
22. J. Hafizovic, M. Bjørgen, U. Olsbye, P. D. C. Dietzel, S. Bordiga, C. Prestipino, C. Lamberti and K. P. Lillerud, *J. Am. Chem. Soc.*, 2007, **129**, 3612-3620.
23. Y. Lee, S. Kim, J. K. Kang and S. M. Cohen, *Chem. Commun.*, 2015, **51**, 5735−5738.
24. S. M. Khopkar, *Analytical Chemistry of Macrocyclic and Supramolecular Compounds*, Narosa Publishing House Pvt. Ltd., 2005.
25. H. Fei and S. M. Cohen, *J. Am. Chem. Soc.*, 2015, **137**, 2191−2194.
26. S. M. Williams, J. S. Brodbelt, A. P. Marchand, D. Cal and K. Mlinaric-Majerski, *Anal. Chem.*, 2002, **74**, 4423−4433.
27. M. J. Katz, Z. J. Brown, Y. J. Colon, P. W. Siu, K. A. Scheidt, R. Q. Snurr, J. T. Hupp and O. K. Farha, *Chem. Commun.*, 2013, **49**, 9449−9451.
28. R. M. Izatt, K. Pawlak, J. S. Bradshaw and R. L. Bruening, *Chem. Rev.*, 1991, **91**, 1721−2085.
29. S. S. Han and W. A. Goddard III, *J. Am. Chem. Soc.*, 2007, **129**, 8422−8423.

30. Y.-W. Li, J. Xu, D.-C. Li, J.-M. Dou, H. Yan, T.-L. Hu and X.-H. Bu, *Chem. Commun.*, 2015, **51**, 14211−14214.

31. T.-L. Hu, H. Wang, B. Li, R. Krishna, H. Wu, W. Zhou, Y. Zhao, Y. Han, X. Wang, W. Zhu, Z. Yao, S. Xiang and B. Chen, *Nat. Commun.*, 2015, **6**, 7328−7336.

Table of Contents Entry